



This discussion paper is/has been under review for the journal Natural Hazards and Earth System Sciences (NHESS). Please refer to the corresponding final paper in NHESS if available.

# Periodic Glacial Lake Outburst Floods threatening the oldest Buddhist monastery in north-west Nepal

J. Kropáček<sup>1,2</sup>, N. Neckel<sup>1</sup>, B. Tyrna<sup>1,3</sup>, N. Holzer<sup>2</sup>, A. Hovden<sup>4</sup>, N. Gourmelen<sup>5,6</sup>, C. Schneider<sup>7</sup>, M. Buchroithner<sup>2</sup>, and V. Hochschild<sup>1</sup>

<sup>1</sup>Department of Geography, University of Tübingen, Ruemelinstr. 19–23, 72070 Tübingen, Germany

<sup>2</sup>Institute for Cartography, Dresden University of Technology, Helmholtzstr. 10, 01069 Dresden, Germany

<sup>3</sup>Geomer GmbH, Im Breitspiel 11b, 69126 Heidelberg, Germany

<sup>4</sup>Department of Culture Studies and Oriental Languages, University of Oslo, Niels Henrik Abels vei 36, 0371 Oslo, Norway

<sup>5</sup>Institut de Physique du Globe de Strasbourg, Université de Strasbourg, 5 rue René Descartes, 67084 Strasbourg CEDEX, France

<sup>6</sup>School of Geosciences, University of Edinburgh, Geography Building Drummond Street, Edinburgh EH8 9XP, UK

<sup>7</sup>Department of Geography, RWTH Aachen University, Templergraben 55, 52056 Aachen, Germany

Title Page

Abstract

Introduction

Conclusions

References

Tables

Figures



Back

Close

Full Screen / Esc

Printer-friendly Version

Interactive Discussion



Received: 15 October 2014 – Accepted: 22 October 2014 – Published: 17 November 2014

Correspondence to: J. Kropáček (jan.kropacek@uni-tuebingen.de)

Published by Copernicus Publications on behalf of the European Geosciences Union.

# NHESSD

2, 6937–6971, 2014

## Periodic GLOF in north-west Nepal

J. Kropáček et al.

Title Page

Abstract

Introduction

Conclusions

References

Tables

Figures



Back

Close

Full Screen / Esc

Printer-friendly Version

Interactive Discussion



## Abstract

Since 2004 Halji Village, home of the oldest Buddhist Monastery in north-west Nepal has suffered from recurrent Glacial Lake Outburst Floods (GLOFs). Studies of recent satellite images identified a supra-glacial lake, located at a distance of 6.5 km from the village, as a possible source of the flood. During a field survey in 2013, the finding was confirmed and several entrances to en-glacial conduits which are draining the lake were found. The topography of the lake basin was then mapped by combining Differential Global Positioning System (DGPS) measurements with a Structure From Motion (SFM) approach from terrestrial photographs. From this model the maximum filling capacity of the lake has been estimated as  $1.06 \times 10^6 \text{ m}^3$  with a maximum discharge of  $77.8 \text{ m}^3 \text{ s}^{-1}$  calculated using an empirical relation. The flooded area in the valley has been estimated by employing a raster-based hydraulic model considering six scenarios of discharge volume and surface roughness. To understand the changes in glacier geometry in the last decade the thinning and retreat of Halji Glacier have been analysed by geodetic mass balance measurements and a time series of satellite images respectively. The GLOF occurrences have further been correlated with cumulative temperature and cumulative liquid precipitation calculated from the High Asia Reanalysis (HAR) dataset. Finally, effective mitigation measures and adaption strategies for Halji village have been discussed.

## 1 Introduction

Glacier thinning and retreat in the Himalayas have resulted in the formation of a number of inherently instable glacial lakes in the region (ICIMOD, 2011; Nie et al., 2013). The sudden catastrophic release of water from such lakes, commonly denoted as a Glacial Lake Outburst Flood (GLOF), leads to extensive damage and often to casualties in the valley downstream (e.g. Haeberli, 1983; Björnsson, 1992; Huggel et al., 2002). Ice-dammed lakes are usually drained through a tunnel incised into the basal ice, by

**NHESSD**

2, 6937–6971, 2014

## Periodic GLOF in north-west Nepal

J. Kropáček et al.

Title Page

Abstract

Introduction

Conclusions

References

Tables

Figures

◀

▶

◀

▶

Back

Close

Full Screen / Esc

Printer-friendly Version

Interactive Discussion



**Periodic GLOF in  
north-west Nepal**

J. Kropáček et al.

Title Page

Abstract

Introduction

Conclusions

References

Tables

Figures

◀

▶

◀

▶

Back

Close

Full Screen / Esc

Printer-friendly Version

Interactive Discussion



ice-marginal drainage or by mechanical failure of a part of the dam (Walder and Costa, 1996). Although it is known that GLOFs occur mainly after the onset of the snow melting season (Haeberli, 1983), reliable prediction of the timing is difficult (Mergili et al., 2011). Further, the mechanisms and circumstances of glacial flood release are still largely unknown (Fountain, 2011). For an estimation of the peak discharge of a tunnel-like drainage an empirical power-law relation was proposed by Clague and Mathews (1973), but its application to other types of floods can lead to significant underestimation (Walder and Costa, 1996). In some cases, the total discharge volume can reach several km<sup>3</sup> (Walder and Costa, 1996), but even discharges as small as 10 m<sup>3</sup> s<sup>-1</sup> can be destructive if they trigger a debris flow (Haeberli, 1983; Driedger and Fountain, 1989).

Since 2004 Halji village in north-west Nepal has been affected by periodic flooding occurring at the beginning of summer. The village is located in the Limi Valley at the southern slopes of the Gurla Mandhata Massif at an altitude of 3740 m a.s.l. (a.s.l.) (1). So far the floods have washed away a substantial part of arable land and damaged several houses on the western margin of the settlement. Rinchenling Monastery, which is located only about 30 m from the damaged zone, plays a central role in the local community and has significant value as cultural heritage (Bidari, 2004; Hovden, 2013). Recent research shows that the monastery dates back to the beginning of the eleventh century (Hovden, 2013) and it is thus one of the oldest Tibetan Buddhist monasteries in Nepal. The whole village is built on a flat alluvial fan of the Halji River (Halji Khola) formed by unconsolidated alluvial sediments. Future flooding thus represents a serious threat to both the village and the monastery.

Limi Valley is located at the southern margin of the Tibetan Plateau. The climate of the region, which can be classified as Dwc after Köppen (Peel et al., 2007), is characterized by cool summers and dry winters. The main climate parameters measured at the closest meteorological station in Burang (3901 m a.s.l.) are shown in Fig. 2. A fast retreat of glaciers in the north-western part of Gurla Mandhata in the last decades was reported by Yao et al. (2007) and Holzer et al. (2014).

**Periodic GLOF in north-west Nepal**

J. Kropáček et al.

Title Page

Abstract

Introduction

Conclusions

References

Tables

Figures



Back

Close

Full Screen / Esc

Printer-friendly Version

Interactive Discussion



The objective of this study is to investigate the supra-glacial lake basin as the source of the flooding and to determine its drainage mechanism. To understand the timing and impact of GLOF events in Halji the maximum discharge is estimated for various filling levels including the maximum level considering the present shape of the basin.

Potentially flooded areas are delimited based on hydraulic modelling. As GLOF events are related to glacier dynamics, a further objective is to investigate the changes in glacier area and volume in the last decade. Glacier thinning and mass balance are estimated by subtraction of two Digital Elevation Models (DEMs), and the glacier retreat is mapped using Landsat images. The GLOF occurrences are compared to major climate parameters derived from the High Asia Reanalysis dataset (HAR), (Mausson et al., 2013). Finally, with regard to possible GLOF events in the future, suitable mitigation measures are briefly discussed.

## 2 History of the GLOFs in Halji

According to interviews with the local villagers, floods were recorded in the years 2004, 2006, 2007, 2008, 2009 and 2011, while in 2005, 2010, 2012, 2013 and 2014 no flooding occurred (Diemberger et al., 2015). All GLOFs in Halji have taken place at the end of June or beginning of July. Whereas the exact dates of the early floods are not known, the timing of the most recent floods is very regular with a time span of 7 days. The reports about the flood intensity in the particular years given by the local inhabitants are somewhat divergent, but the magnitude of the flood seems to have increased over time. The flood on 30 June 2011, which was the largest so far, is well documented by photos and videos taken by one of the authors, who was an eye-witness to the event. The stream level in the village rose early in the afternoon and stayed high for several hours. The glacier flood triggered a debris flow which covered the bottom of the valley with a layer of sediment reaching several metres of thickness at some places (Fig. 1).

After the first floods some technical measures were considered in order to prevent future damage of the settlement. In 2010, a gabion wall was constructed along the east

bank of the stream above and in the village. Its damaged parts were replaced after the flood in 2011 and further extensions of the wall were made in 2014.

After the flood in 2009, a team of local villagers attempted a climb of the glacier in order to search for the source of the flood. They reported that they discovered a small lake partly covered by ice (Diemberger et al., 2015). High resolution satellite imagery acquired in November 2011 available through Bing Maps (<http://www.bing.com/maps/>), revealed a lake basin like structure on the northern side of the glacier tongue. Examination of this imagery suggested that the basin could be filled by melt water forming a supra-glacial lake with sufficient volume to cause the flood subsequent to a sudden drainage.

### 3 Materials and methods

#### 3.1 Identification of the lake and mapping of the glacier extent from satellite data

In order to identify the source of the flooding we checked a number of satellite image archives for the period from April to September. The number of useful images for this period turned out to be drastically limited due to persistent cloud cover related to the Monsoon. The lake could be detected only on a handful of Landsat images.

To understand the circumstances of the GLOF events, changes in the extent of the Halji Glacier in the last decade were mapped using two cloud-free satellite images from Landsat-7 with a ground resolution of 30 m. The scenes were acquired by Enhanced Thematic Mapper Plus (ETM+) on 13 October 2001 and 26 November 2011. The glacier body was delimited using a band ratio of bands 5 and 3 (i.e. RED/SWIR) and subsequent threshold application following Paul and Kääb (2005), which is an effective approach also in shadowed areas. As the scene from 2011 shows some “SLC-off” artefacts (NASA, 2004) manual editing was needed to eliminate narrow data gaps crossing the glacier.

Title Page

Abstract

Introduction

Conclusions

References

Tables

Figures



Back

Close

Full Screen / Esc

Printer-friendly Version

Interactive Discussion



## 3.2 Mapping of the lake basin topography

In order to provide a robust base for a detailed lake basin morphometry, the empty lake was surveyed by means of 130 Differential Global Positioning System (DGPS) measurements. The measurements were conducted in and around the basin in stop-and-go mode with a reference station on solid rock. Additionally, a dense point cloud was generated from a Structure From Motion (SFM) approach (Snavely et al., 2008; Westoby et al., 2012).

For this we employed the freely available VisualSFM software (e.g. Wu, 2011). As an input we used 161 images taken during the 2013 field campaign with an off-shelf *Pentax K100D Super* camera. The great advantage of the SFM technique compared to conventional photogrammetry is that scene geometry, camera positions and orientation are solved automatically by a redundant approach based on automatically detected features in the overlapping images (Snavely et al., 2008; Westoby et al., 2012). In a first processing step VisualSFM creates a sparse point-cloud and shows the approximated camera positions in a graphical interface (Fig. 3a). In a second processing step a dense point-cloud is generated. As no Ground Control Points (GCPs) were used so far the dense point-cloud is referenced to a relative coordinate system. In order to translate the dense point-cloud to a metric coordinate system we employed seven GCPs acquired by DGPS at the same time the images were taken. Here we used the freely available SFMgeoref Matlab package provided by James and Robson (2012). As the dense point-cloud consists of millions of points we only used the mean value of points on a 1 m × 1 m grid for interpolating the Lake Basin DEM (LB DEM). Next to the SFM points we included 124 DGPS measurements in the final interpolation (Fig. 3b) leaving 6 DGPS measurements unemployed for an accuracy assessment of the final LB DEM. Compared to the well distributed reference DGPS measurements the LB DEM shows a mean and standard deviation of  $0.22 \pm 0.54$  m.

The DEM of the lake basin allowed us to calculate the maximum filling capacity of the basin by summation of differences of the lake bottom elevations to the theoretical

Title Page

Abstract

Introduction

Conclusions

References

Tables

Figures



Back

Close

Full Screen / Esc

Printer-friendly Version

Interactive Discussion



maximum lake elevation level and its multiplication by the pixel size of the LB DEM. The lowest point of the ice barrier was identified as maximum lake level elevation. To characterize the filling process, a hypsographic curve was generated. Peak discharge was calculated for various filling levels applying the power-law formula for tunnel-like discharge through an ice barrier proposed by Clague and Mathews (1973) as:

$$Q_{\max} = 75V_{\max}^{0.67} \quad (1)$$

where  $V_{\max}$  is the discharged volume.

### 3.3 Hydrodynamic modelling of GLOF scenarios

To study the dynamics of the outburst flood events and to assess the flood risk for Halji village and the monastery, the hydrodynamic two-dimensional model FloodArea<sup>HPC</sup> (Assmann et al., 2007; Geomer, 2012) was used to model different GLOF scenarios (Table 1). The influence of input parameters was estimated by a sensitivity analysis and for validation purposes the model outputs were compared to the observations of the 2011 GLOF event. FloodArea<sup>HPC</sup> is a raster-based hydrodynamic model that was developed as an ArcGIS extension to model inundation areas for fluvial flooding, pluvial flooding, flash flooding and dam breaks. It is based on the Manning–Strickler formula and calculates flood depths in a cell by cell approach (Assmann et al., 2007). Due to the fact that nobody ever witnessed the drainage of the lake during a flood event, there is no data available to simulate a specific event, like the 2011 flooding. Although numerical approaches can be used to model an outburst hydrograph for glacier dammed lakes (Vincent et al., 2010; Westoby et al., 2014), such models could not be applied in our case because most of the necessary parameters like drainage tunnel size, temperature or filling level of the lake are unknown. Therefore, we decided to deal with this parameter uncertainty by modelling different scenarios using a set of parameters (Table 1). This approach enables us to assess the flood hazard for Halji village by delineating potentially flooded areas for different scenarios and estimating parameter

Title Page

Abstract

Introduction

Conclusions

References

Tables

Figures

◀

▶

◀

▶

Back

Close

Full Screen / Esc

Printer-friendly Version

Interactive Discussion



sensitivity for a better understanding of the GLOF dynamics. A high resolution Pléiades DEM (described below) was used to provide detailed information on topography of the valley bottom. To approximate an outflow hydrograph for the scenarios, a Gaussian normal distribution was fitted to the outflow volumes and associated peak flows  $Q_{\max}$ .

### 3.4 Geodetic glacier mass balance from Pléiades satellite imagery

Geodetic glacier mass balances (Fig. 4) were determined for the period 1999 to 2013 by subtracting Shuttle Radar Topography Mission (SRTM) elevations from a more recent DEM derived from Pléiades tri-stereo imagery. Pléiades is a French high resolution earth observation system composed of two satellites launched in 2011 and 2012. It offers in-track tri-stereoscopic image acquisition with a spatial resolution of 0.5 m (panchromatic) and a pixel depth of 12-bit (Astrium, 2012). Imagery of the study site was acquired on 26 October 2013.

We extracted a DEM at 1 m spatial resolution using the PCI 2013 Geomatica Ortho-engine software package and its Rational Functions model. DEM extraction is based on ephemeris information and GCPs. This DEM was used for the hydrodynamic modelling. For the DEM differencing both DEMs were re-sampled to a resolution of 30 m. Elevation pixels with an insufficient stereo matching score ( $< 0.3$ ) were ignored. DEM co-registration to the SRTM reference is based on an analytical approach following Nuth and Kääb (2011) with remaining inaccuracies of 1.24 m in  $X$  and 1.50 m in  $Y$ . We observed a spatially varying elevation bias in form of a slight tilt with respect to SRTM. This was corrected by a two-dimensional linear trend surface to reduce the mean height offset on stable terrain to zero (Holzer et al., 2014).

Outlier detection and gap filling in the difference image to SRTM was employed independently for each glacier accumulation zone and each 25 m elevation band in the ablation zone following Holzer et al. (2014). The accumulation area is separated by an ELA altitude which was estimated as 5660 m a.s.l. for a nearby glacier (G081393E30265N) by Shi (2008). Pixel values outside of the 5 and 95 % quantiles were considered as outliers and similar as for data voids filled by a mean value. Penetration of the SRTM

Title Page

Abstract

Introduction

Conclusions

References

Tables

Figures

◀

▶

◀

▶

Back

Close

Full Screen / Esc

Printer-friendly Version

Interactive Discussion



Title Page

Abstract

Introduction

Conclusions

References

Tables

Figures

I◀

▶I

◀

▶

Back

Close

Full Screen / Esc

Printer-friendly Version

Interactive Discussion



C-band beam into glacier ice was corrected by a depth of 2.3 m for firn and snow (accumulation area) as well as 1.7 m for clean ice (ablation area) with an uncertainty of  $\pm 0.6$  m (Kääb et al., 2012). Glacier thinning and mass balance at a presumed ice density of  $850 \pm 60 \text{ kg m}^{-3}$  (Huss, 2013) was determined for Halji Glacier as well as its two neighbouring glaciers located further to the west. The precision of the DEM was estimated at 4.83 m in form of the Normalized Median Absolute Deviation (NMAD) (Höhle and Höhle, 2009).

### 3.5 Correlation of GLOF occurrence with climate data

Hourly precipitation and temperature in 2 m above the surface were derived from the HAR dataset. The data correspond to a model cell representing the elevation of 5273 m a.s.l. located 4 km from the glacier to the west (Fig. 1). The model contains gridded fields of atmospheric variables with a resolution of 10 km for the Tibetan Plateau and surroundings (Maussion et al., 2013). Following the idea of a degree day model (Braithwaite, 1984) the hourly above zero temperatures of the cell were cumulated for the period from January to June for each year between 2001 and 2011. The end of June corresponds to the outbursts of the lake. The cumulative temperature thus represents a proxy for the volume of melt water amount discharging from the glacier to the lake. Similarly, hourly precipitation from January to June ( $P_{\text{cum}}$ ) was cumulated for temperatures above  $0^\circ\text{C}$  representing liquid precipitation that contributes to the filling of the lake. The two variables  $T_{\text{cum}}$  and  $P_{\text{cum}}$  were compared with the flood occurrences.

## 4 Results

### 4.1 Field campaign in November 2013

During the field campaign in November 2013 the existence of the temporary supraglacial lake indicated by the satellite imagery was proved. A large empty basin was

Title Page

Abstract

Introduction

Conclusions

References

Tables

Figures

I◀

▶I

◀

▶

Back

Close

Full Screen / Esc

Printer-friendly Version

Interactive Discussion



found at the north side of the glacier tongue close to the terminus. Its bottom was covered by a thin layer of lacustrine sediments (Fig. 5b). Moreover, several entrances to en-glacial conduits were discovered along the south-eastern bottom edge of the basin at an altitude of 5292 m a.s.l. The entrances were partially covered by snow and sediments and their total cross-section was estimated as ranging from 5 to 15 m<sup>2</sup>. Close to the entrance the channels were filled with ice forming a horizontal level showing that the channels were blocked and filled with water before the freeze-up. These conduits drain the lake towards an outflow on the south-eastern edge of the glacier covering a distance of 500 m. The entrances clearly follow a sheer crack predisposed probably by a discontinuity between ice layers. This is in agreement with findings of Fountain et al. (2005) and Gulley (2009) who showed that en-glacial conduits in temperate glaciers follow glacio-structural features such as ice fractures rather than developing a passage through the ice mass of a higher conductivity as presumed in the past (Shreve, 1972).

## 4.2 Evidences of the lake basin on satellite imagery

The first evidence of an ice-dammed basin on the Halji Glacier was found on aerial images from the archive of the Survey Department in Kathmandu photographed in 1996. However the structure was covered by snow and it is not possible to say whether it contained a lake or not. The lake could be detected only on Landsat images from 8 June 2007 acquired by Thematic Mapper (TM), and from 5 and 21 June 2009 acquired by Enhanced Thematic Mapper (ETM+) (Fig. 6, Table 2). For seven Landsat scenes acquired mainly in September it could be stated that the lake was not present. The rest of the Landsat images as well as other available high resolution images were either cloud covered or showed snow-covered surfaces where the lake basin is located.

## 4.3 Geometric properties of the lake basin and peak discharge

The morphology of the lake basin as reconstructed by DGPS and SFM is shown in Fig. 3. It appears that the glacier ice barrier that blocks the basin is 24 m high at its

lowest point. To understand the relation between the lake depth and its volume, a hypsometric curve was derived for the basin (Fig. 7). The maximum volume of the basin before the overtopping of the barrier in the south-east is  $1.06 \times 10^6 \text{ m}^3$ . The lake area, volume and peak discharge calculated after Clague and Mathews (1973) is given in Table 3. The area of the glacier that drains to the lake basin is  $1.12 \text{ km}^2$  and the whole basin including off-glacier area is  $1.46 \text{ km}^2$ .

#### 4.4 Flow discharge and flood extent

The discharge curves generated by the model FloodArea<sup>HPC</sup> are shown in Fig. 8. It can be seen that the slope of the falling limb of the discharge curve is much steeper than the rising limb in all scenarios. Travel time, defined as the period between the outflow peak and the arrival of the flood wave peak at the village, is about three hours for all scenarios. Peak discharge at the village is roughly the same as the input peak discharge at the outflow of the lake. Against our expectations, there is almost no attenuation of the flood wave magnitude between the outflow and the village. Only a shift of the peak towards the end of the flood wave can be detected (Fig. 8). As expected, higher roughness (Strickler coefficient =  $15 \text{ m}^{1/3} \text{ s}^{-1}$ ) increases travel time, which means that the onset of the flood at Halji village begins about 15–30 min later than with a roughness value of  $20 \text{ m}^{1/3} \text{ s}^{-1}$  (Fig. 8c). Concerning the timing of the peak flow, however, this effect is not strong. Roughness values also have no effect on flood extents. So it can be concluded that the choice of the roughness parameter is not of crucial importance.

The extents of the flooded area for 50, 75 and 100 % of the lake filling capacity using a roughness value of  $15 \text{ m}^{1/3} \text{ s}^{-1}$  are shown in Fig. 8. The flooded areas calculated with a roughness value of  $20 \text{ m}^{1/3} \text{ s}^{-1}$  are almost identical and are therefore not shown. A flood induced by 50 % of the lake volume seems not large enough to cause severe damage to the village. Flooding of the housing area can be observed in the scenarios with an input of 75 and 100 % of the lake volume.

Title Page

Abstract

Introduction

Conclusions

References

Tables

Figures



Back

Close

Full Screen / Esc

Printer-friendly Version

Interactive Discussion



## 4.5 Thinning and retreat of the Halji Glacier in the last decade

The change in extent of the Halji Glacier in the period 2001 to 2011 is shown in Fig. 10. The glacier front retreated for up to about 80 m in the vicinity of the lake. The changes in glacier thickness for the period 1999–2013 are shown in Fig. 4. Table 4 presents changes in glacier mean elevation and in total ice volume as well as the mean annual mass balance for the Halji glacier and two other glaciers located further to the west.

## 4.6 Correlation of GLOF events with climate data

The comparison of the occurrence of the GLOF with the hourly cumulative above zero temperature (Fig. 10a) shows a good match. Starting in 2003, the years with no flood appear to have a low  $T_{cum}$ . A similar pattern is present in the case of  $P_{cum}$ , although the dependency seems to be weaker. The high value of  $P_{cum}$  for the year 2011 corresponds to the strongest flood recorded so far.

The cumulated liquid precipitation gives us an idea if the supra-glacial lake can be filled by mere precipitation amount received in the drainage basin of the lake. The theoretical runoff from the lake basin disregarding the re-freezing ranges from  $0.50 \times 10^6 \text{ m}^3$  to  $0.93 \times 10^6 \text{ m}^3$ . The latter value represents the so far strongest flood in 2011. This amount corresponds to 88 % of the maximum filling volume of the lake.

## 5 Discussion

The appearance of the supra-glacial lake on the Halji Glacier can be linked to the overall glacier retreat in the Himalayas in the last decades (Kääb et al., 2012; Gardelle et al., 2013; Neckel et al., 2014). The evolution of the lake was likely induced by an undulation of the glacier surface that reflects an over-deepening of the glacier bed. The presence of the basin before the first GLOF event is not well documented due to a striking absence of useful satellite data. The long life of the supra-glacial basin is probably

Title Page

Abstract

Introduction

Conclusions

References

Tables

Figures

◀

▶

◀

▶

Back

Close

Full Screen / Esc

Printer-friendly Version

Interactive Discussion



a result of a balance between glacier movement, glacier thinning and enlargement of the basin by thermal dissipation of the lake water.

The lake basin can fill up relatively quickly during June as documented by two Landsat images for the year 2007. The flood occurred each time within a range of a few days at the end of June/beginning of July. This suggests that the floods are rather climate driven than triggered by extreme precipitation events. This is further supported by the coincidence of the GLOF events with high values of cumulative above zero temperature calculated from the HAR dataset. It was shown that the lake basin can almost fill up merely with liquid precipitation accumulated until the end of June. Snow and glacier melting during June is also depending on temperature. This means that in each year with a relatively warm June a GLOF event may occur. The satellite images from May 2013 and June 2014 suggest that during the years without GLOF no lake develops in the basin. In these years water from the drainage area above the basin probably drains sub-glacially.

The entrances to the conduits found in the lake basin suggest that the lake discharge flows first en-glacially and further probably sub-glacially. This mechanism can be classified as a tunnel-like discharge that could be described for different filling levels by an empirical equation. It should be noted that the maximum discharges computed can be largely exceeded if the conduits get blocked and then suddenly released as described by Ballantyne and McCann (1980) and Haeberli (1983). This means that larger floods than the maximum calculated cannot be ruled out.

The simulation of the flooded area did not result in a complete flooding of the village. However, we observed during the field trip that houses in Halji are built on loose sediments of an alluvial fan. As such they are threatened by undercutting of the river bank by the flood. This mechanism led to a collapse of two of the houses next to the river during the flood in 2011. The monastery can be affected either by undercutting or if the stream loaded by sediment spills over the gabion wall and enters the alleys of the settlement. In this respect, one of the alleys is especially dangerous as it is in-

## Periodic GLOF in north-west Nepal

J. Kropáček et al.

Title Page

Abstract

Introduction

Conclusions

References

Tables

Figures



Back

Close

Full Screen / Esc

Printer-friendly Version

Interactive Discussion



clined towards the village center and leads from the river bank directly to the monastery (Fig. 9).

Assuming a continuation of the glacier retreat detected from Landsat data and the negative mass balance in the future the lake basin will eventually disappear due to the downwasting of the glacier leading to the elimination of the GLOF hazard for Halji Village. However it is possible that the size of the lake basin and the associated discharge volume still increase due to thermal dissipation of water before the predicted decline of the basin.

## 6 Conclusions

The presented study shows how a combination of field measurements and satellite data analysis can help to assess risks connected to the evolution of a glacial lake. The lake that seasonally develops on the Halji Glacier is relatively small compared to the large moraine dammed lakes in Nepal. Nevertheless, its discharge which is connected to releases of debris flows presents a serious threat to both Halji Village and the ancient Rinchenling Monastery.

It appears that even under present climate conditions the glacier will further retreat, a development which will eventually lead to the decline of the lake basin. Nevertheless, it seems likely that the basin will persist at least for several more years. Therefore suitable mitigation measures should be considered to improve the flood resilience of Halji Village.

Taking into account the size of the ice barrier and the depth of the basin, an artificial drainage of the lake appears to be difficult and due to the inaccessibility and remoteness of the place almost impossible to achieve. Instead, a further reinforcement of the riverbank in the village and upstream is recommended. A simple measure to prevent the flood would be an ascent to the lake basin around mid-June to check visually whether the lake develops. This would provide valuable information about a possible burst. Further an early warning system for Halji Village should be considered.

Title Page

Abstract

Introduction

Conclusions

References

Tables

Figures

◀

▶

◀

▶

Back

Close

Full Screen / Esc

Printer-friendly Version

Interactive Discussion



Title Page

Abstract

Introduction

Conclusions

References

Tables

Figures

I◀

▶I

◀

▶

Back

Close

Full Screen / Esc

Printer-friendly Version

Interactive Discussion



*Acknowledgements.* This work was supported by the German Research Foundation (DFG) Priority Programme 1372, “Tibetan Plateau: Formation–Climate–Ecosystems” within the DynRG-TiP (“Dynamic Response of Glaciers on the Tibetan Plateau to Climate Change”) project under the code BU 949/20-3 and SCHN 680/3-3, and by the German Federal Ministry of Education and Research (BMBF) Program “Central Asia–Monsoon Dynamics and Geo-Ecosystems” (CAME) within the WET project (“Variability and Trends in Water Balance Components of Benchmark Drainage Basins on the Tibetan Plateau”) under the codes 03G0804D, 03G0804E and 03G0804F.

Pléiades imagery was received by the Institut de Physique du Globe and the ICube Laboratory (UMR 7357 CNRS) of the University of Strasbourg as part of the second call of the program RTU (Recette Thématique Utilisateurs) within the satellite program ORFEO (Optical and Radar Federation for Earth Observation) of the French Space Agency CNES and processed by the Institute of Cartography of the Dresden University of Technology, Germany (<https://rtu-pleiades.kalimsat.eu>).

The Landsat scenes were provided by the USGS and the SRTM-3 C-band DEM version 4.1 by the Consultative Group for International Agricultural Research (CGIAR). We thank the community of Halji and Benjamin Schröter from TU Dresden for their support during the field trip. Thanks to Gebhard Warth for his support with Landsat data processing. We acknowledge support by Open Access Publishing Fund of the University of Tuebingen.

## References

- Assmann, A., Schroeder, M., and Hristov, M.: *Angewandte Geoinformatik 2007, Beiträge zum 19. AGIT-Symposium*, chap. High Performance Computing for raster based modelling, Salzburg, 4–6 July 2007, 19–24, 2007. 6944
- Astrium: *Pléiades Imagery – User Guide V2.0*, Astrium GEO-Information Services, France, 5, rue des Satellites, BP 14359, 31030 Toulouse Cedex 4, France, 2012. 6945
- Ballantyne, C. and McCann, S.: Short-lived damming of a high-Arctic ice-marginal stream, Ellesmere Island, N. W. T., Canada, *J. Glaciol.*, 25, 487–491, 1980. 6950
- Bidari, K.: Halji Monastery – a hidden heritage in North-West Nepal, *Ancient Nepal*, 155, 1–5, 2004. 6940

**Periodic GLOF in north-west Nepal**

J. Kropáček et al.

Title Page

Abstract

Introduction

Conclusions

References

Tables

Figures

I◀

▶I

◀

▶

Back

Close

Full Screen / Esc

Printer-friendly Version

Interactive Discussion



- Björnsson, H.: Jökulhaups in Iceland: prediction, characteristics and simulation, *Ann. Glaciol.*, 16, 95–106, 1992. 6939
- Braithwaite, R. J.: Calculation of degree-days for glacier-climate research, *Z. Gletscherk. Glazialgeol.*, 20, 1–8, 1984. 6946
- 5 Clague, J. J. and Mathews, W. H.: The magnitude of jökulhaups, *J. Glaciol.*, 12, 501–504, 1973. 6940, 6944, 6948
- Diemberger, H., Hovden, A., and Yeh, E.: The honour of the mountains is the snow: Tibetan livelihoods in a changing climate (forthcoming), in: *The High-Mountain Cryosphere: Environmental Changes and Human Risks*, edited by: Huggel, C., Carey, M., Clague, J. J., and Kääh, A., Cambridge University Press, Cambridge, 2015. 6941, 6942
- 10 Driedger, C. and Fountain, A.: Glacier outburst floods at Mount Rainier, Washington state, USA, *Ann. Glaciol.*, 13, 51–55, 1989. 6940
- Fountain, A.: Englacial processes, in: *Encyclopedia of Snow, Ice and Glaciers*, Springer, Dordrecht, the Netherlands, 1253 pp., 2011. 6940
- 15 Fountain, A., Jacobel, R., Schlichting, R., and Jansson, P.: Fractures as the main pathways of water flow in temperate glaciers, *Nature*, 433, 618–621, 2005. 6947
- Gardelle, J., Berthier, E., Arnaud, Y., and Kääh, A.: Region-wide glacier mass balances over the Pamir-Karakoram-Himalaya during 1999–2011, *The Cryosphere*, 7, 1263–1286, doi:10.5194/tc-7-1263-2013, 2013. 6949
- 20 Geomer: FloodArea User Manual V. 10.0, 49 pp., Heidelberg, 2012. 6944
- Gulley, J.: Structural control of englacial conduits in the temperate Matanuska Glacier, Alaska, USA, *J. Glaciol.*, 55, 681–690, 2009. 6947
- Haerberli, W.: Frequency and characteristics of glacier floods in the Swiss Alps, *Ann. Glaciol.*, 4, 85–90, 1983. 6939, 6940, 6950
- 25 Höhle, J. and Höhle, M.: Accuracy assessment of digital elevation models by means of robust statistical methods, *ISPRS J. Photogramm.*, 64, 398–406, doi:10.1016/j.isprs.2009.02.003, 2009. 6946
- Holzer, N., Neckel, N., Buchroithner, M., Gourmelen, N., Colin, J., and Bolch, T.: Glacier variations at Gurla Mandhata (Naimona'nyi), Tibet: a multi-sensoral approach including TanDEM-X, Pléiades and KH-7 Gambit-1, *Remote Sens. Environ.*, under review, 2014. 6940, 6945
- 30 Hovden, A.: Who were the sponsors? Reflections on recruitment and ritual economy in three Himalayan village monasteries, in: *Tibetans who Escaped the Historian's Net: Studies in the*

Title Page	
Abstract	Introduction
Conclusions	References
Tables	Figures
◀	▶
◀	▶
Back	Close
Full Screen / Esc	
Printer-friendly Version	
Interactive Discussion	



Social History of Tibetan Societies, Vajra Publications, edited by: Ramble, C., Schwieger, P., and Travers, A., Kathmandu, 209–230, 2013. 6940

Huggel, C., Kääb, A., Haeberli, W., Teysseire, P., and Paul, F.: Remote sensing based assessment of hazards from glacier lake outbursts: a case study in the Swiss Alps, *Can. Geotech. J.*, 39, 316–330, 2002. 6939

Huss, M.: Density assumptions for converting geodetic glacier volume change to mass change, *The Cryosphere*, 7, 877–887, doi:10.5194/tc-7-877-2013, 2013. 6946

ICIMOD: Glacial Lakes and Glacial Lake Outburst Floods in Nepal, Tech. rep., ICIMOD, Kathmandu, 2011. 6939

James, M. R. and Robson, S.: Straightforward reconstruction of 3D surfaces and topography with a camera: accuracy and geoscience application, *J. Geophys. Res.*, 117, 2156–2202, 2012. 6943

Kääb, A., Berthier, E., Nuth, C., Gardelle, J., and Arnaud, Y.: Contrasting patterns of early twenty-first-century glacier mass change in the Himalayas, *Nature*, 488, 495–498, doi:10.1038/nature11324, 2012. 6946, 6949

Maussion, F., Scherer, D., Mölg, T., Collier, M., Curio, J., and Finkelburg, R.: Precipitation seasonality and variability over the Tibetan Plateau as resolved by the high Asia reanalysis, *J. Climate*, 27, 1910–1927, 2013. 6941, 6946

Mergili, M., Schneider, D., Worni, R., and Schneider, J.: Glacial lake outburst floods in the Pamir of Tajikistan: challenges in prediction and modelling, in: 5th International Conference on Debris-Flow Hazards Mitigation: Mechanics, Prediction and Assessment, edited by: Genevois, R., Hamilton, D. L., and Prestininzi, A., Padua, Sapienze Università Editrice university press, 973–982, ISBN 978-88-95814-46-9, doi:10.4408/IJEGE.2011-03.B-106, 2011. 6940

NASA: Landsat 7 science data users handbook, NASA, available at: [http://landsathandbook.gsfc.nasa.gov/pdfs/Landsat7\\_Handbook.pdf](http://landsathandbook.gsfc.nasa.gov/pdfs/Landsat7_Handbook.pdf) (last access: 8 September 2014), 2004. 6942

Neckel, N., Kropáček, J., Bolch, T., and Hochschild, V.: Glacier mass changes on the Tibetan Plateau 2003–2009 derived from ICESat laser altimetry measurements, *Environ. Res. Lett.*, 9, 014009, doi:10.1088/1748-9326/9/1/014009, 2014. 6949

Nie, Y., Liu, Q., and Liu, S.: Glacial lake expansion in the Central Himalayas by Landsat images, 1990–2010, *PLoS ONE*, 8, e83973, doi:10.1371/journal.pone.0083973, 2013. 6939

Title Page	
Abstract	Introduction
Conclusions	References
Tables	Figures
◀	▶
◀	▶
Back	Close
Full Screen / Esc	
Printer-friendly Version	
Interactive Discussion	



Nuth, C. and Kääb, A.: Co-registration and bias corrections of satellite elevation data sets for quantifying glacier thickness change, *The Cryosphere*, 5, 271–290, doi:10.5194/tc-5-271-2011, 2011. 6945

Paul, F. and Kääb, A.: Perspectives on the production of a glacier inventory from multispectral satellite data in Arctic Canada: Cumberland Peninsula, Baffin Island, *Ann. Glaciol.*, 42, 59–66, 2005. 6942

Peel, M. C., Finlayson, B. L., and McMahon, T. A.: Updated world map of the Köppen-Geiger climate classification, *Hydrol. Earth Syst. Sci.*, 11, 1633–1644, doi:10.5194/hess-11-1633-2007, 2007. 6940

Shi, Y.: *Concise Glacier Inventory of China*, Shanghai Popular Science Press, Shanghai, 2008. 6945

Shreve, R.: Movement of water in glaciers, *J. Glaciol.*, 11, 205–214, 1972. 6947

Snavely, N., Seitz, S. M., and Szeliski, R.: Modeling the world from internet photo collections, *Int. J. Comput. Vision*, 80, 189–210, doi:10.1007/s11263-007-0107-3, doi:10.1007/s11263-007-0107-3, 2008. 6943

Vincent, C., Auclair, S., and Meur, E.: Outburst flood hazard for glacier-dammed Lac de Rochemelon, France, *J. Glaciol.*, 56, 91–100, doi:10.3189/002214310791190857, 2010. 6944

Walder, J. S. and Costa, J.: Outburst floods from glacier-dammed lakes: the effect of mode of lake drainage on flood magnitude, *Earth Surf. Proc. Land.*, 21, 701–723, 1996. 6940

Westoby, M., Brasington, J., Glasser, N., Hambrey, M., and Reynolds, J.: “Structure-from-Motion” photogrammetry: a low-cost, effective tool for geoscience applications, *Geomorphology*, 179, 300–314, doi:10.1016/j.geomorph.2012.08.021, 2012. 6943

Westoby, M. J., Brasington, J., Glasser, N. F., Hambrey, M. J., Reynolds, J. M., and Hassan, M. A. A. M.: Numerical modelling of Glacial Lake Outburst Floods using physically based dam-breach models, *Earth Surf. Dynam. Discuss.*, 2, 477–533, doi:10.5194/esurf-d-2-477-2014, 2014. 6944

Wu, C.: VisualSFM: A Visual Structure from Motion System, available at: <http://ccwu.me/vsfm/> (last access: 11 November 2014), 2011. 6943

Yao, T.-D., Pu, J., Tian, L., Yang, W., Duan, K., Ye, Q., and Lonnie, G. T.: Recent Rapid Retreat of the Naimona’nyi Glacier in Southwestern Tibetan Plateau, *J. Glaciol. Geocryol.*, 29, 503–508, 2007. 6940

## Periodic GLOF in north-west Nepal

J. Kropáček et al.

**Table 1.** GLOF model scenarios considering various discharge volumes and surface roughness values.

scenario	% of lake volume	total discharge volume (m <sup>3</sup> )	$Q_{\max}$ (m <sup>3</sup> s <sup>-1</sup> )	Time to peak (h)	Roughness (m <sup>1/3</sup> s <sup>-1</sup> )
S1	100	1 056 000	77.8	5	20
S2	75	792 000	64.2	5	20
S3	50	528 000	48.9	5	20
S4	100	1 056 000	77.8	5	15
S5	75	792 000	64.2	5	15
S6	50	528 000	48.9	5	15

Title Page

Abstract

Introduction

Conclusions

References

Tables

Figures

◀

▶

◀

▶

Back

Close

Full Screen / Esc

Printer-friendly Version

Interactive Discussion



## Periodic GLOF in north-west Nepal

J. Kropáček et al.

**Table 2.** Dates of glacier lake presence detected on Landsat images and occurrence of GLOF in respective years.

–	GLOF	lake before 1 Jul	no lake
2004	yes	–	–
2005	–	–	6 Sep
2006	yes	–	9 Sep
2007	yes	8 Jun	12 Sep
2008	yes	–	–
2009	23 Jun	5, 21 Jun	17 Sep
2010	–	–	28 Sep
2011	30 Jun	–	–
2012	–	–	–
2013	–	–	23 May
2014	–	–	3 Jun

Title Page

Abstract

Introduction

Conclusions

References

Tables

Figures

◀

▶

◀

▶

Back

Close

Full Screen / Esc

Printer-friendly Version

Interactive Discussion



## Periodic GLOF in north-west Nepal

J. Kropáček et al.

**Table 3.** Area, volume and peak discharge for different water levels in the basin calculated using the LB DEM.

elevation (m a.s.l.)	level (m)	area (m <sup>2</sup> )	volume (10 <sup>6</sup> m <sup>3</sup> )	$Q_{\max}$ (m <sup>3</sup> s <sup>-1</sup> )
5297	5	6368	0.03	6.33
5302	10	12 552	0.12	17.70
5307	15	24 280	0.29	32.97
5312	20	43 684	0.63	55.22
5316	24	64 328	1.06	77.81

Title Page

Abstract

Introduction

Conclusions

References

Tables

Figures

◀

▶

◀

▶

Back

Close

Full Screen / Esc

Printer-friendly Version

Interactive Discussion



## Periodic GLOF in north-west Nepal

J. Kropáček et al.

Title Page

Abstract

Introduction

Conclusions

References

Tables

Figures

◀

▶

◀

▶

Back

Close

Full Screen / Esc

Printer-friendly Version

Interactive Discussion



**Table 4.** Glacier mean elevation and total ice volume changes as well as annual glacier mass balances measured from DEM differencing of SRTM-3 (1999) to Pléiades (2013).

Glacier/GLIMS ID	Mean elevation change (m)	Volume change (Gt × 10 <sup>-3</sup> )	Annual mass balance (m w.e. a <sup>-1</sup> )
Halji Glacier	-6.6 ± 4.9	-15.8 ± 11.6	-0.40 ± 0.30
G081437E30281N	-13.9 ± 4.9	-92.0 ± 32.9	-0.84 ± 0.30
G081393E30265N	-3.2 ± 4.9	-18.8 ± 28.7	-0.19 ± 0.30

## Periodic GLOF in north-west Nepal

J. Kropáček et al.

Title Page

Abstract

Introduction

Conclusions

References

Tables

Figures

◀

▶

◀

▶

Back

Close

Full Screen / Esc

Printer-friendly Version

Interactive Discussion



**Table 5.** Liquid precipitation amount  $V$  received in the area draining to the supra-glacial lake each year until the end of Jun which was calculated using hourly precipitation and temperature data from the HAR.

year	$V$ ( $10^6 \text{ m}^3$ )
2001	0.51
2002	0.93
2003	0.71
2004	0.67
2005	0.90
2006	0.70
2007	0.60
2008	0.84
2009	0.46
2010	0.39
2011	0.94

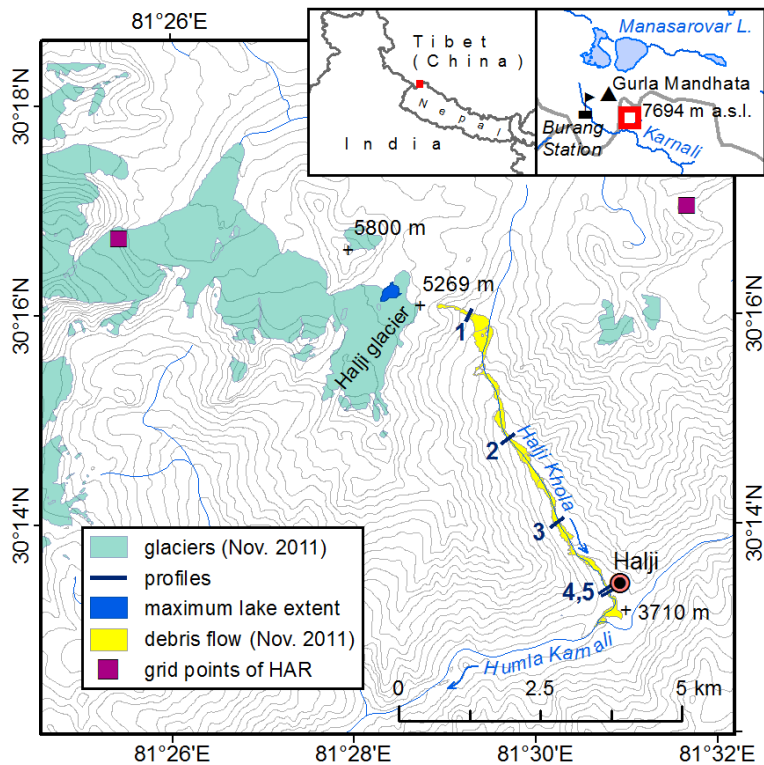


**Figure 1.** Overview map of the study area. The extent of the debris flow was delineated from a high resolution image from November 2011 available on Bing Maps.

**Periodic GLOF in north-west Nepal**

J. Kropáček et al.

Discussion Paper | Discussion Paper | Discussion Paper | Discussion Paper | Discussion Paper

Title Page	
Abstract	Introduction
Conclusions	References
Tables	Figures
◀	▶
◀	▶
Back	Close
Full Screen / Esc	
Printer-friendly Version	
Interactive Discussion	



## Periodic GLOF in north-west Nepal

J. Kropáček et al.

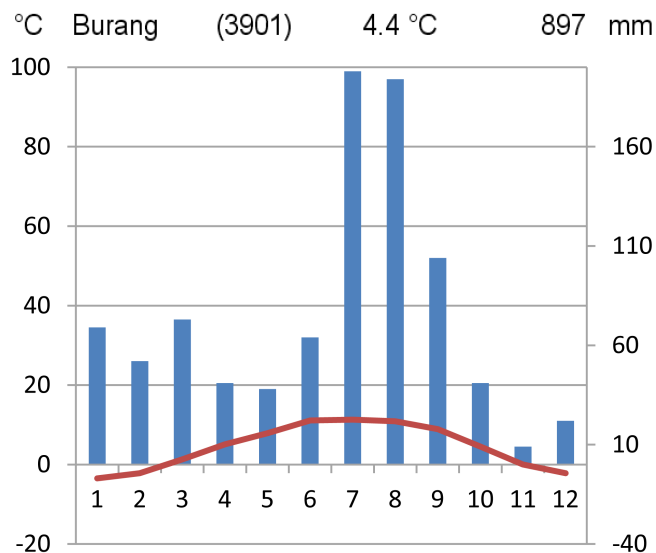


**Figure 2.** Climate diagram of Burang station located 30 km west from Halji Glacier (<http://en.climate-data.org/location/495449/>). Precipitation is indicated by the blue columns and temperature by the red curve.

Title Page

Abstract

Introduction

Conclusions

References

Tables

Figures

◀

▶

◀

▶

Back

Close

Full Screen / Esc

Printer-friendly Version

Interactive Discussion



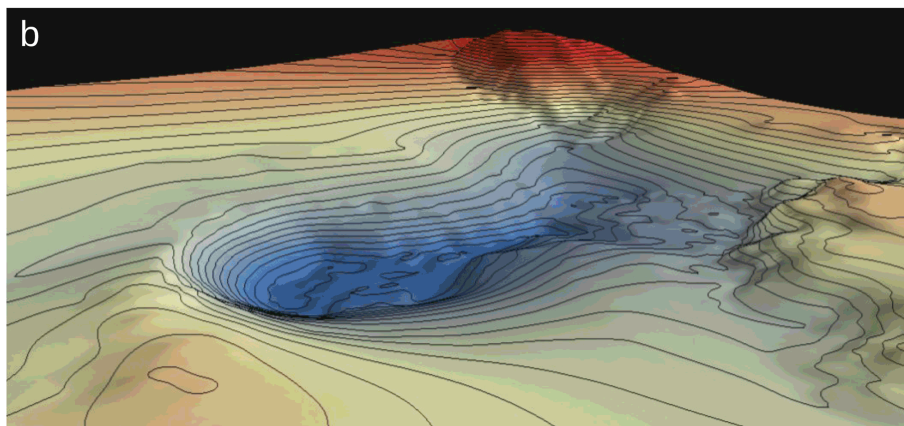
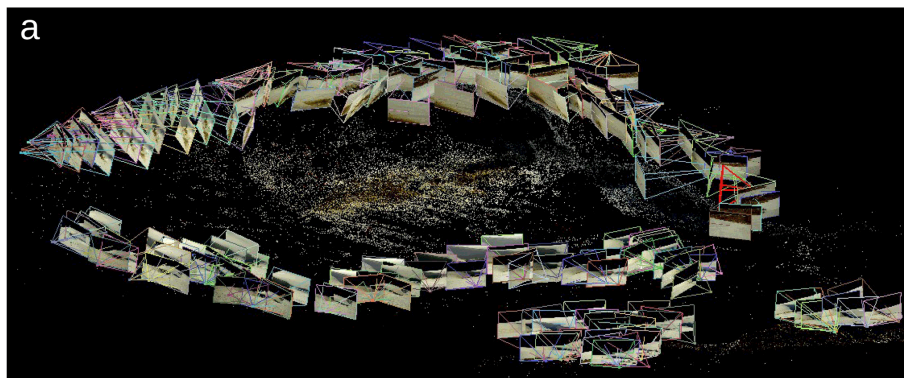


**Figure 3.** Terrain reconstruction of the lake basin using Structure From Motion (SFM) and Differential Global Positioning System (DGPS) measurements. **(a)** Perspective view of the sparse point-cloud and camera positions as seen from the North. **(b)** Interpolated Lake Basin DEM (LB DEM) and contour lines as seen from the north-east.

## Periodic GLOF in north-west Nepal

J. Kropáček et al.

Title Page

Abstract

Introduction

Conclusions

References

Tables

Figures

◀

▶

◀

▶

Back

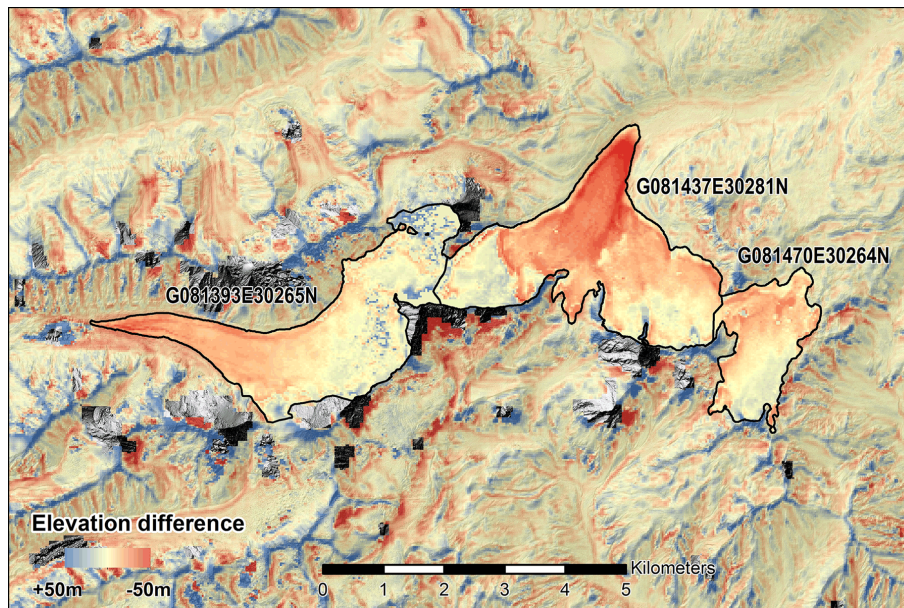
Close

Full Screen / Esc

Printer-friendly Version

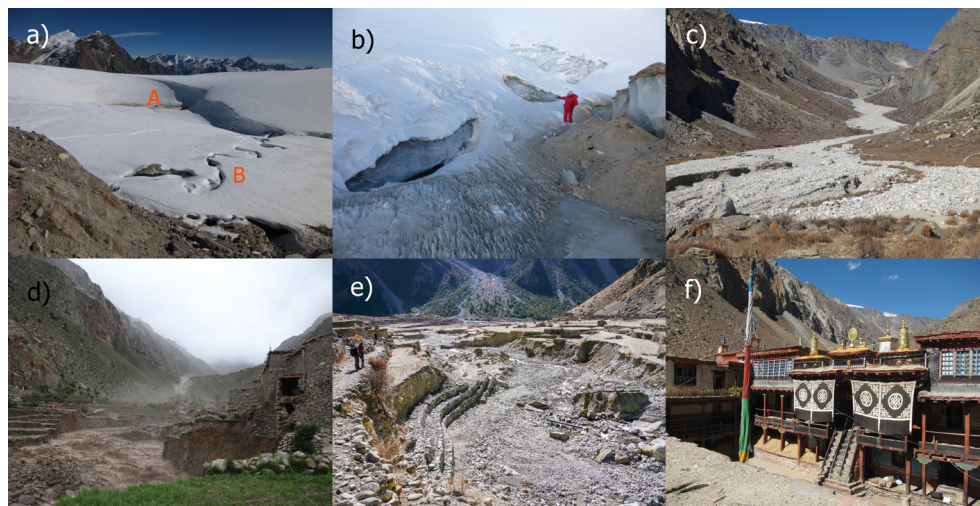
Interactive Discussion





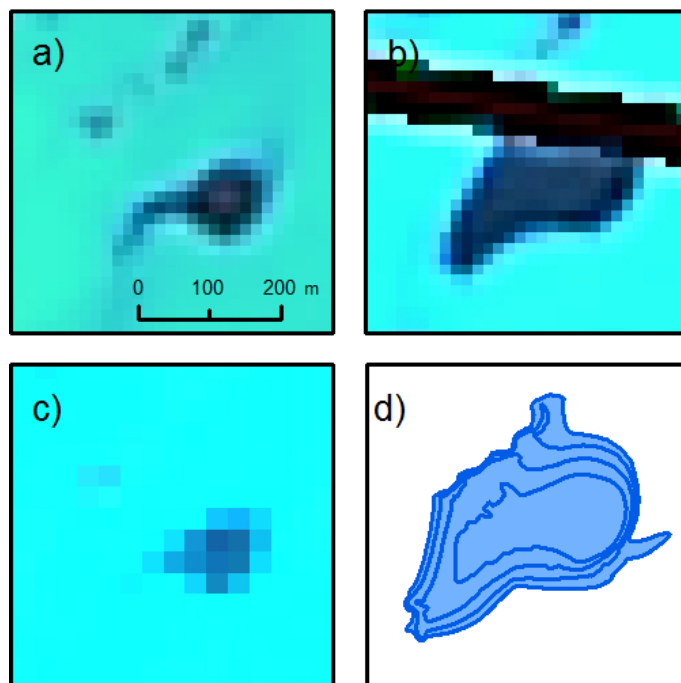
**Figure 4.** Difference image of Pléiades DEM (2013) minus SRTM DEM (1999) for mass balance calculation of glaciers G081470E30264N (Halji Glacier), G081437E30281N and G081393E30265N (Glacier IDs are from Randolph Glacier Inventory).

[Title Page](#)[Abstract](#)[Introduction](#)[Conclusions](#)[References](#)[Tables](#)[Figures](#)[I ◀](#)[▶ I](#)[◀](#)[▶](#)[Back](#)[Close](#)[Full Screen / Esc](#)[Printer-friendly Version](#)[Interactive Discussion](#)



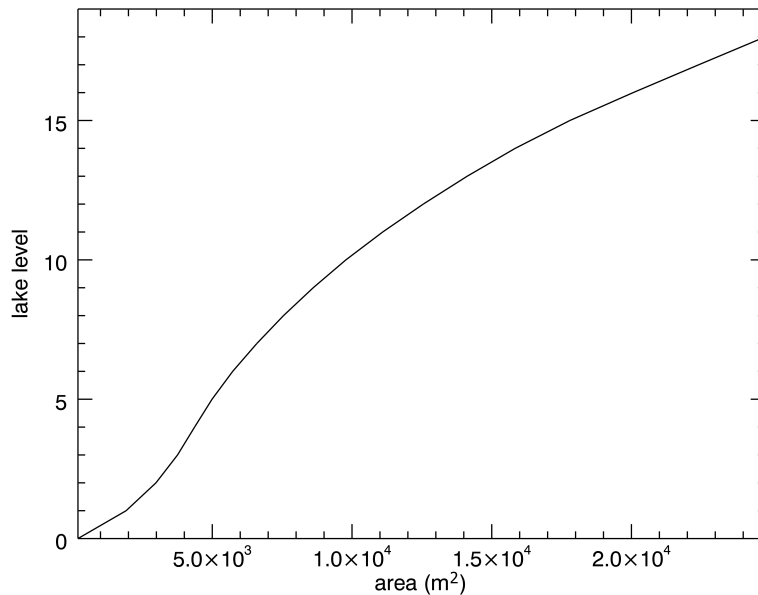
**Figure 5.** View of the empty lake basin from the north **(a)**. The entrances to the en-glacial conduits draining the lake located at the lower edge of the toe of the ice barrier are marked by A. The supra-glacial streams which lead melt water to the basin are marked by B. A detailed view of the entrances to the en-glacial conduits is shown in **(b)**. A layer of the lacustrine sediment is visible in the lower right corner. Debris deposited by the floods in the middle part of the valley is presented in **(c)**. Collapsed houses in Halji village after the flood on 30 June 2011 are captured in **(d)**. Eroded banks of Halji Khola at Halji village was reinforced by a gabion wall (photo taken in November 2013) **(e)**. The Halji glacier can be seen on the horizon above Rinchenling monastery in **(f)**.

[Title Page](#)
[Abstract](#)
[Introduction](#)
[Conclusions](#)
[References](#)
[Tables](#)
[Figures](#)
[◀](#)
[▶](#)
[◀](#)
[▶](#)
[Back](#)
[Close](#)
[Full Screen / Esc](#)
[Printer-friendly Version](#)
[Interactive Discussion](#)

**Figure 6.** The supra-glacial lake on Landsat images (RGB combination of bands 5, 4 and 3) acquired on 8 June 2007 **(a)**, 24 June 2007 **(b)** and 5 June 2009 **(c)**. The image from 24 June 2007 is affected by a data gap due to “SLC-off” artefacts. Lake extents corresponding to 25, 50 and 100 % of the maximum filling capacity are shown in **(d)**.

[Title Page](#)[Abstract](#)[Introduction](#)[Conclusions](#)[References](#)[Tables](#)[Figures](#)[I ◀](#)[▶ I](#)[◀](#)[▶](#)[Back](#)[Close](#)[Full Screen / Esc](#)[Printer-friendly Version](#)[Interactive Discussion](#)



**Figure 7.** Hypsographic curve of the lake basin showing the relation of the lake depth and the lake area.

**Periodic GLOF in north-west Nepal**

J. Kropáček et al.

Title Page

Abstract Introduction

Conclusions References

Tables Figures

◀ ▶

◀ ▶

Back Close

Full Screen / Esc

Printer-friendly Version

Interactive Discussion



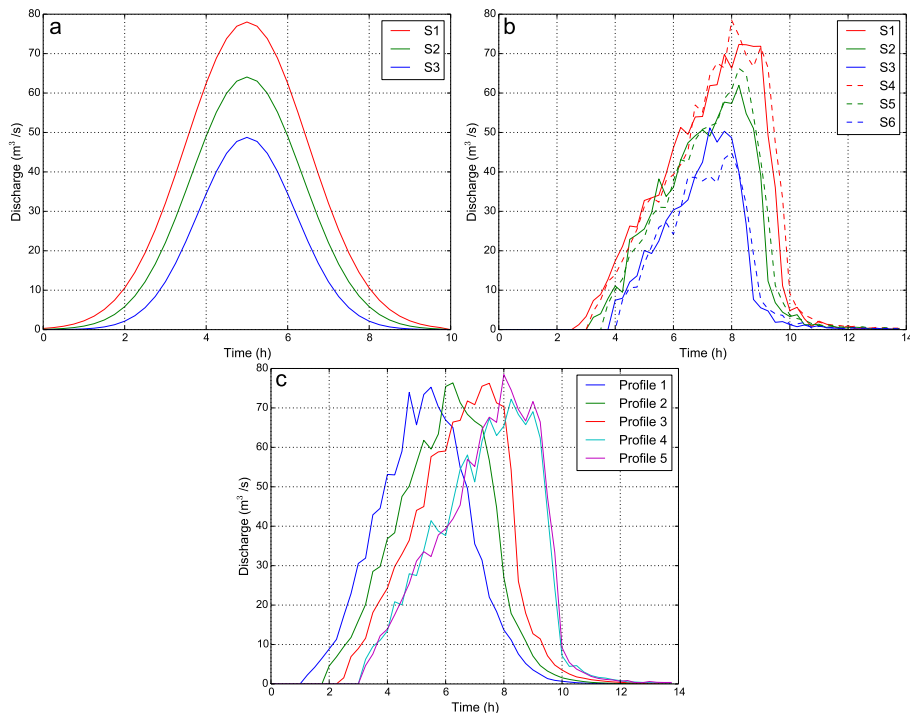


**Figure 8.** (a) Lake outflow hydrographs for three different filling levels (100, 75 and 50 % of lake volume) which were used as input for the hydrodynamic modelling. (b) Modelled discharge curves for Profile 5 next to the village for different lake volumes and different roughness parameters according to Table 1 (for the location of Profile 5 see Figs. 1 and 9); (c) modelled discharge curves of S1 scenario for profiles 1–5 show the downstream propagation of the flood wave.

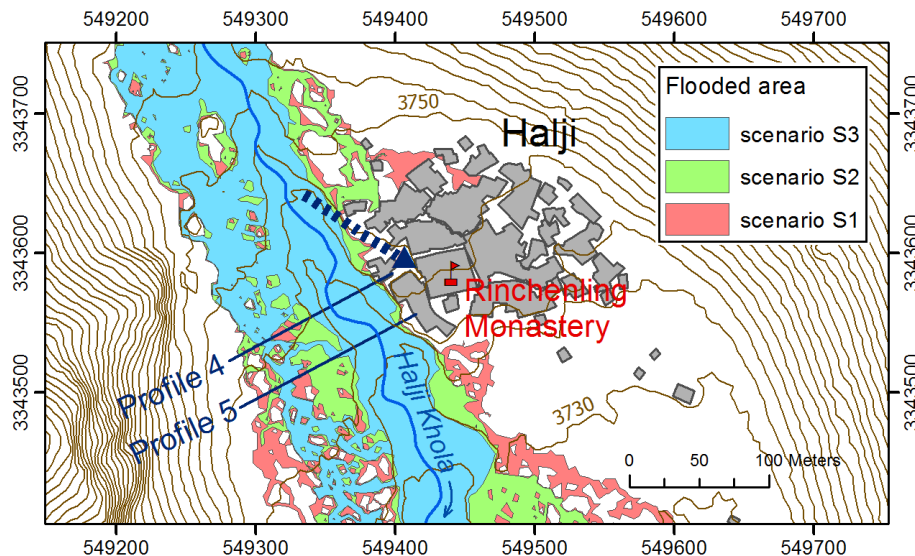


**Figure 9.** Flooded area in the vicinity of Halji Village assuming three different peak discharge values and roughness value of 20. The passage between houses leading to the monastery is shown as a dashed blue arrow.

[Title Page](#)[Abstract](#)[Introduction](#)[Conclusions](#)[References](#)[Tables](#)[Figures](#)[◀](#)[▶](#)[◀](#)[▶](#)[Back](#)[Close](#)[Full Screen / Esc](#)[Printer-friendly Version](#)[Interactive Discussion](#)

## Periodic GLOF in north-west Nepal

J. Kropáček et al.

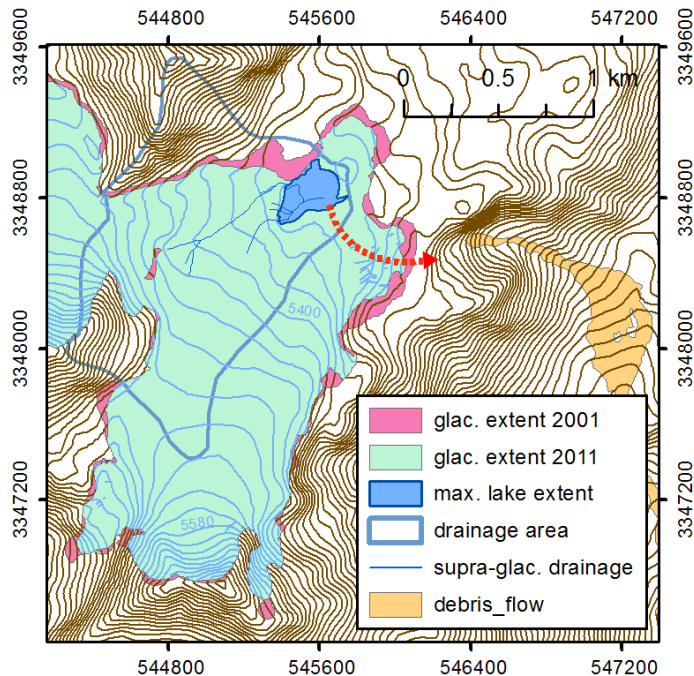


**Figure 10.** Changes in the extent of the Halji Glacier in the period from 2001 to 2011 as detected from Landsat images. Drainage of the supra-glacial lake during the GLOF event is shown as a dashed red arrow.

Title Page

Abstract

Introduction

Conclusions

References

Tables

Figures

◀

▶

◀

▶

Back

Close

Full Screen / Esc

Printer-friendly Version

Interactive Discussion



## Periodic GLOF in north-west Nepal

J. Kropáček et al.

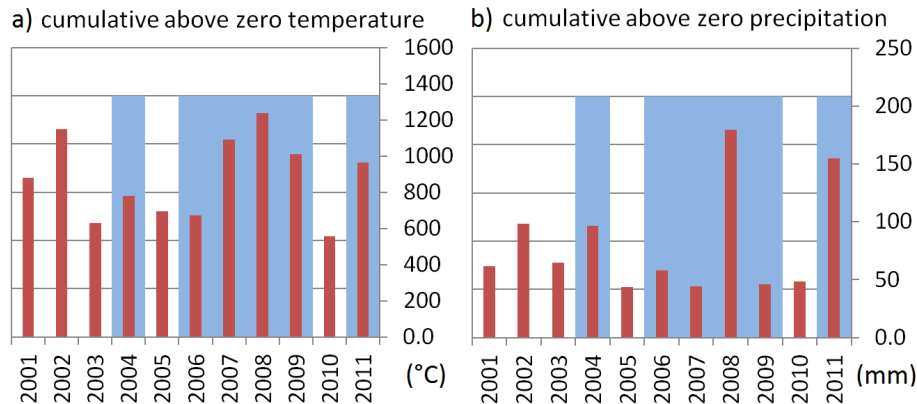


**Figure 11.** Cumulative above zero temperature  $T_{cum}$  (a) and precipitation  $P_{cum}$  (b) calculated for the period January to June derived from hourly HAR data. The precipitation was cumulated only for above zero temperatures thus it represents the liquid part of precipitation. The years with a GLOF event are marked by a blue column in the background.

Title Page

Abstract

Introduction

Conclusions

References

Tables

Figures

◀

▶

◀

▶

Back

Close

Full Screen / Esc

Printer-friendly Version

Interactive Discussion

